MATHEMATICAL ENGINEERING
TECHNICAL REPORTS

Global Optimization of Robust Truss Topology via Mixed Integer Semidefinite Programming

Kazuo YONEKURA and Yoshihiro KANNO

METR 2009–25 June 2009

DEPARTMENT OF MATHEMATICAL INFORMATICS
GRADUATE SCHOOL OF INFORMATION SCIENCE AND TECHNOLOGY
THE UNIVERSITY OF TOKYO
BUNKYO-KU, TOKYO 113-8656, JAPAN

WWW page: http://www.keisu.t.u-tokyo.ac.jp/research/techrep/index.html

Global Optimization of Robust Truss Topology via Mixed Integer Semidefinite Programming

Kazuo Yonekura † and Yoshihiro Kanno ‡

Department of Mathematical Informatics,
University of Tokyo, Tokyo 113-8656, Japan

Abstract

This paper discusses a global optimization method of robust truss topology under the load uncertainties and lower bound constraints of the member cross-sectional areas. We consider a non-stochastic uncertainty model of external loads, and attempt to minimize the maximum compliance corresponding to the most critical load. A design-dependent uncertainty model of external loads is proposed in order to consider the variation of truss topology rigorously. It is shown that this optimization problem can be formulated as a 0–1 mixed integer semidefinite programming (0–1MISDP) problem. We propose a branch-and-bound method for computing the global optimal solution of the 0–1MISDP. Numerical examples illustrate that the topology of robust optimal truss depends on the magnitude of uncertainty.

Keywords

Topology optimization; Robust optimization; Semidefinite program; Global optimization, Branch-and-bound method.

1 Introduction

There have been various methods for the topology optimization of trusses [1–4, 6, 14, 19]. Many of those methods are based on the ground structure method, in which the member cross-sectional areas are regarded as continuous nonnegative variables in the process of optimization and the optimal topology is obtained by removing the members with vanishing cross-sectional areas. However, it is well known that the optimal solution obtained by such an approach often has very thin members, which are not acceptable for the practical point of view. For overcoming this defect, Achtziger and Stolpe [2, 3, 4] considered the optimization problem with the discrete member cross-sectional areas. Ohsaki and Katoh [19] explicitly considered positive lower bounds for member cross-sectional areas.

As another difficulty in the conventional truss topology optimization, it is known that the optimum solution is often kinematically indeterminate (kinematically unstable). For example, consider a ground structure of the 22-member plane truss illustrated in Figure 1. The three nodes on the left side are fixed, while the bottom-right node is loaded by the vertical external force. The optimum solution obtained by minimizing the compliance is shown in Figure 2, which is kinematically

†E-mail: kazuo_yonekura@mist.i.u-tokyo.ac.jp.

‡Corresponding author. Address: Department of Mathematical Informatics, Graduate School of Information Science and Technology, University of Tokyo, Bunkyo, Tokyo 113-8656, Japan. E-mail: kanno@mist.i.u-tokyo.ac.jp. Phone: +81-3-5841-6906, Fax: +81-3-5841-6886.

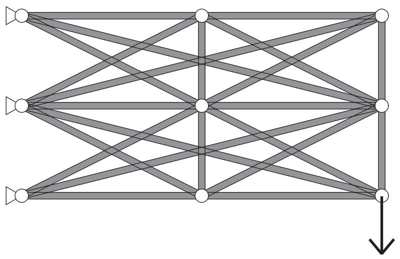

Figure 1: A 22-member ground structure.

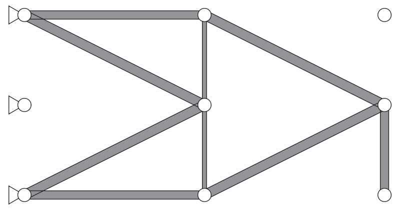

Figure 2: The optimal solution of the 22-member truss without considering load uncertainties.

indeterminate. Note that the kinematical indeterminacy of a truss is determined as follows. Let $D \in \mathbb{R}^{n \times m}$, $\boldsymbol{q} \in \mathbb{R}^m$ and $\boldsymbol{f} \in \mathbb{R}^n$ denote the equilibrium matrix, the vector of member axial forces, and the external load vector, respectively. The equilibrium condition is written as

$$D\boldsymbol{q} = \boldsymbol{f}.$$

The kinematical indeterminacy is determined in terms of the rank of the matrix D as follows.

- $\operatorname{rank} D < n \;\Rightarrow$ kinematically unstable;
- $\operatorname{rank} D = n \;\Rightarrow$ kinematically stable.

In Figure 2 we see that $\operatorname{rank} D = 9$ and $n = 10$, and hence this optimal solution is kinematically unstable. The optimum topology is unstable because we do not consider any uncertainties of the external load but only the nominal one.

The observation above implies that we have to take uncertain loads into consideration in order to obtain a kinematically stable structure. Ben-Tal and Nemirovski [9] proposed a method for truss optimization considering load uncertainties based on the *semidefinite program* (SDP). In this approach, firstly, it is required to specify the set of existing nodes, at which the uncertain loads are supposed to be applied. Secondly, the robust optimal truss is obtained by minimizing the maximum value of the compliance among the uncertain loads. Therefore all the nodes specified at the first step of the procedure remain at the obtained optimal solution, and hence it is often that the truss topology does not change drastically. Moreover, the obtained solution may include some additional nodes other than specified ones, if we suppose that uncertain loads are applied only at some of nodes of the ground structure. The obtained solution is in general kinematically unstable in such a case, because no uncertain load is supposed to be applied at the additional nodes. Thus it is difficult to specify in advance the set of existing nodes at the robust optimal solution. In this paper we overcome this difficulty by considering the design-dependent uncertainty set of external loads; see section 3.1 for details.

In [9] a heuristic method was also proposed to specify the existing nodes at the first step of their approach, i.e. considering only the nominal load we firstly solve the conventional minimization problem of the compliance for a ground structure with sufficiently large number of nodes, then for the robust optimization we define another ground structure having only the remaining nodes at the nominal optimal solution. However, this heuristic method cannot find the global optimal solution of the robust topology optimization in general; see sections 5.2 and 5.3 for examples of such cases.

Methodologies as well as numerical techniques for robust structural design have received increasing attention recently, because structures built in the real-world always have various uncertainties caused by manufacture errors, limitation of knowledge of input disturbance, etc. Based on the probabilistic uncertainty model, various methods have been well-developed for reliability-based optimization [10, 23]. However, it is often difficult to estimate those parameters accurately. Hence it is also important to develop methods for robust structural optimization based on the non-probabilistic uncertainty framework. By using the so-called convex model approach [8] to non-probabilistic uncertainty model, numerical algorithms were proposed for robust structural optimization [5, 20]. A min-max formulation of a robust compliance design was presented for continua [11]. Kočvara *et al.* [16] considered a free-material design under multiple loadings by using a cascading technique. Matsuda and Kanno [18] considered a robust structural optimization with the specified worst-case plastic limit load factor under the load uncertainties, and proposed a linear programming reformulation. Based on the robustness function defined in the info-gap decision theory [7], Kanno and Takewaki [15] performed a maximization of the level of robustness of a structure under the load uncertainty.

In this paper, we propose a global optimization method for the robust truss topology optimization by minimizing the compliance corresponding to the most critical external load. For dealing with the variation of truss topology rigorously, we propose a design-dependent uncertainty model of external loads. We show that this optimization problem can be formulated as a 0–1 *mixed integer semidefinite programming* (0–1MISDP) problem, i.e. a semidefinite programming problem in which some variables are subjected to be binary constraint conditions. A branch-and-bound method is proposed for computing the global optimal solution of the 0–1MISDP, at each iteration of which we solve a linear SDP problem by using the primal-dual interior-point method. It is well known that the computational efficiency of a branch-and-bound method highly depends on the node selection strategy and the branching rule; see, e.g. [12]. We propose a node selection strategy and a branching rule, as well as a heuristic method for finding an upper bound solution, for our particular 0–1MISDP arising from the context of robust structural optimization.

This paper is organized as follows. In section 2, we present the nominal topology optimization problem of trusses with the positive lower bound constraints of member cross-sectional areas in order to avoid thin members. In section 3, we present a topology-dependent uncertainty model of external loads, and formulate a robust topology optimization of trusses as a 0–1MISDP. The proposed 0–1MISDP is solved globally by using the branch-and-bound method, the details of which are described in section 4. Numerical results are presented in section 5, where we show that the robust optimal topology of a truss depends on the level of uncertainty. Some conclusions are drawn in section 6.

A few words regarding our notation: all vectors are assumed to be column vectors. The $(m+n)$-dimensional column vector $(\boldsymbol{u}^\top, \boldsymbol{v}^\top)^\top$ consisting of $\boldsymbol{u} \in \mathbb{R}^m$ and $\boldsymbol{v} \in \mathbb{R}^n$ is often written simply as $(\boldsymbol{u}, \boldsymbol{v})$. We denote by $\mathbb{R}^n_+ \subset \mathbb{R}^n$ the nonnegative orthant defined by $\mathbb{R}^n_+ = \{\boldsymbol{x} = (x_i) \in \mathbb{R}^n \mid x_i \geq 0 \ (i = 1, \dots, n)\}$. For vectors $\boldsymbol{p} = (p_i) \in \mathbb{R}^n$ and $\boldsymbol{q} = (q_i) \in \mathbb{R}^n$, we write $\boldsymbol{p} \geq \boldsymbol{0}$ and $\boldsymbol{p} \geq \boldsymbol{q}$ if $\boldsymbol{p} \in \mathbb{R}^n_+$ and $\boldsymbol{p} - \boldsymbol{q} \in \mathbb{R}^n_+$, respectively. We denote by $\mathcal{S}^n$ the set of $n \times n$ real symmetric matrices. We write $X \succeq O$ if $X \in \mathcal{S}^n$ is positive semidefinite.

2 Topology optimization with binary variables

In this section we formulate a conventional truss topology optimization which attempts to minimize the compliance under the lower bound constraints on the cross-sectional areas of the existing members, in which we suppose that only the nominal external load is applied.

2.1 Compliance minimization for nominal external load

Consider a truss with the fixed locations of nodes and the members that can exist. Let $\boldsymbol{f} \in \mathbb{R}^n$ denote the external load vector, where n is the number of degrees of freedom of displacements. We denote by $\boldsymbol{a} \in \mathbb{R}^m$ the vector of member cross-sectional areas, where m is the number of members. The displacements vector $\boldsymbol{u} \in \mathbb{R}^n$ is found from the system of equilibrium equations,

$$K(\boldsymbol{a})\boldsymbol{u} = \boldsymbol{f}. \tag{1}$$

Here $K(\boldsymbol{a})$ denotes a stiffness matrix which is positive semidefinite and written in the form of

$$K(\boldsymbol{a}) = \sum_{i=1}^{m} a_i K_i,$$

where K_i $(i = 1, \dots, m)$ are positive semidefinite constant matrices.

Consider the minimization problem of the compliance, which is one of measures of structural stiffness. The compliance, c, is defined as the external work, i.e.

$$\begin{aligned} c(\boldsymbol{a}; \boldsymbol{f}) &= \boldsymbol{f}^\top \boldsymbol{u} \\ &= \sup_{\boldsymbol{u} \in \mathbb{R}^n} \{2\boldsymbol{f}^\top \boldsymbol{u} - \boldsymbol{u}^\top K(\boldsymbol{a})\boldsymbol{u}\}. \end{aligned} \tag{2}$$

The stationary condition of (2) reads

$$\boldsymbol{f} - K(\boldsymbol{a})\boldsymbol{u} = \boldsymbol{0},$$

which is equivalent to (1). This implies that the optimal solution of the minimization problem of the compliance satisfies (1). Hence, it is not necessary to consider the equilibrium equations, (1), as the explicit equality constraint conditions in the optimization problem.

Let $\boldsymbol{l}$ denote the vector of member lengths. The upper bound constraint of the structural volume is written as

$$\boldsymbol{l}^\top \boldsymbol{a} \le \bar{V}, \tag{3}$$

where $\bar{V}$ is the specified upper bound of structural volume.

Let $\tilde{\boldsymbol{f}}$ denote the nominal value, or the best estimate, of $\boldsymbol{f}$. From (2) and (3), the minimization problem of the compliance associated with the nominal external load is formulated as

$$\begin{aligned} \text{(TO)}: \quad \min_{\tau, \boldsymbol{a}} \quad & \tau & \text{(4a)} \\ \text{s.t.} \quad & \tau \ge c(\boldsymbol{a}; \tilde{\boldsymbol{f}}), & \text{(4b)} \\ & \boldsymbol{l}^\top \boldsymbol{a} \le \bar{V}, & \text{(4c)} \\ & \boldsymbol{a} \ge \boldsymbol{0}, & \text{(4d)} \end{aligned}$$

where τ and $\boldsymbol{a}$ are the variables. It is not recommended to solve the problem (TO) directly because the constraint condition (4b) is not easy to deal with. Hence, various equivalent formulation have been proposed for (TO), e.g. [1, 6, 14].

2.2 Constraints on member cross-sectional areas

In this section we introduce the lower bound constraints of the member cross-sectional areas in order to avoid thin members which cannot be accepted practically.

Note that some members are removed from the ground structure in the process of optimization. Hence, the cross-sectional area of each member should be either equal to zero or larger than the specific lower bounds. This condition is written as

$$a_i = 0 \ \text{ or } \ a_{\min} \le a_i \le a_{\max}, \qquad \forall i, \tag{5}$$

where $a_{\min}$ and $a_{\max}$ are the specified lower and upper bounds of cross-sectional areas, respectively. Note that if it is not necessary to consider the upper bound constraints, we may assign $a_{\max}$ with a large enough value so that the upper bound constraints become redundant. By using a 0–1 variable t_i, we can rewrite (5) as

$$a_i \begin{pmatrix} 1 \\ -1 \end{pmatrix} \le t_i \begin{pmatrix} a_{\max} \\ -a_{\min} \end{pmatrix}, \quad t_i \in \{0, 1\}, \qquad \forall i. \tag{6}$$

Indeed, if $t_i = 0$, then (6) is reduced to

$$0 \le a_i \le 0 \quad \Leftrightarrow \quad a_i = 0.$$

On the other hand, if $t_i = 1$, then (6) is reduced to

$$a_{\min} \le a_i \le a_{\max}.$$

Thus we can see that (6) is equivalent to (5). Note that, in (6), the binary variable t_i plays a role of an indicator of the existence of the ith member.

3 Robust topology optimization considering load uncertainties

In section 3.1 we consider the minimization problem of the maximum compliance, which is shown to be formulated as a 0–1MISDP. The minimization problem of structural volume under the upper bound constraint on the maximum compliance is presented in section 3.2. Section 3.3 shows that the global optimum solution is obtained by solving the 0–1MISDP presented in section 3.1.

3.1 Minimization problem of maximum compliance

Although in the problem (TO) we suppose only a nominal external load $\tilde{\boldsymbol{f}}$, an actual structure can be subjected to various unexpected loads. In order to represent the unexpected uncertain loads, we first revisit the uncertainty model of the external loads proposed in [9].

Define $Q \in \mathbb{R}^{n \times \ell}$ by

$$Q = (\tilde{\boldsymbol{f}}, r\boldsymbol{v}_1, r\boldsymbol{v}_2, \dots, r\boldsymbol{v}_{\ell-1}), \tag{7}$$

where $\boldsymbol{v}_j$ $(j = 1, \dots, \ell - 1)$ are orthonormal basis vectors of the orthogonal complement of $\tilde{\boldsymbol{f}}$, $r \in \mathbb{R}_+$ is a constant representing the level of uncertainty, and ℓ is the number of degrees of the freedom of displacements corresponding to the nodes at which the uncertain external forces are supposed to be applied. Note that it is usually natural to put $\ell = n$. The uncertainty set, $\bar{\mathcal{F}} \subseteq \mathbb{R}^n$, of the external loads is defined by

$$\bar{\mathcal{F}} = \{Q\boldsymbol{e} \mid 1 \geq \|\boldsymbol{e}\|\}, \tag{8}$$

which represents an ellipsoid in the n-dimensional space. The external load, $\boldsymbol{f}$, is assumed to be running through $\bar{\mathcal{F}}$, i.e.

$$\boldsymbol{f} \in \bar{\mathcal{F}}. \tag{9}$$

It is emphasized that uncertain loads can be applied to all the nodes in the uncertainty model defined by (8) and (9), and hence each node should remain at the optimal solution. This situation is not natural because, in the ground structure method, the topology should drastically change and some nodes should be removed. This motivates us to consider an alternative uncertainty model such that if the kth node is removed, i.e. there exists no member connected to the kth node, then the uncertain loads cannot be applied to the kth node.

Let $\mathcal{J}_k \subset \mathcal{J}$ denote the set of indices of degrees of freedom of displacements of the kth node, where $\mathcal{J} = \{1, \dots, n\}$. In order to guarantee that no uncertainty loads are applied to the vanishing nodes, we introduce a 0–1 variable p_j which represents the existence of the corresponding node. If there exists no member connected to the kth node then the kth node should be removed and we put $p_j = 0$ $(j \in \mathcal{J}_k)$, while if the kth node remains then we put $p_j = 1$ $(j \in \mathcal{J}_k)$. More precisely, p_j is related to the existence of the kth node as follows.

Condition 1.

(i) At least one member is connected to the kth node $\Rightarrow$ the node k should remain, and $p_j = 1$ $(j \in \mathcal{J}_k)$;

(ii) $\exists j \in \mathcal{J}_k : \tilde{f}_j \neq 0$, i.e. the nominal external load is applied to the kth node $\Rightarrow$ the node k should remain, and $p_j = 1$ $(j \in \mathcal{J}_k)$;

(iii) Otherwise, the kth node is removed, and $p_j = 0$ $(j \in \mathcal{J}_k)$.

Let $\mathrm{diag}(\boldsymbol{p})$ denote the $n \times n$ diagonal matrix with a vector $\boldsymbol{p}$ satisfying Condition 1 on its diagonal. If the kth node disappears in the process of topology optimization, then any uncertain external load should not be applied to the kth node. Observe that this condition is satisfied by the external load vector defined by $\boldsymbol{f} = \mathrm{diag}(\boldsymbol{p})Q\boldsymbol{e}$ for any $\boldsymbol{e} \in \mathbb{R}^\ell$. Hence, we define the uncertainty set, $\mathcal{F}(\boldsymbol{p}) \subseteq \mathbb{R}^n$, of the external loads by

$$\mathcal{F}(\boldsymbol{p}) = \{\mathrm{diag}(\boldsymbol{p})Q\boldsymbol{e} \mid \boldsymbol{e} \in \mathbb{R}^\ell,\ 1 \geq \|\boldsymbol{e}\|\}, \tag{10}$$

instead of $\bar{\mathcal{F}}$ in (8), and we consider all possible external loads satisfying $\boldsymbol{f} \in \mathcal{F}(\boldsymbol{p})$ for the robust optimization. Note that the uncertainty set $\mathcal{F}(\boldsymbol{p})$ defined in (10) depends on the truss topology, which enables us to deal with the change of topology rigorously in the process of optimization. Consider the maximum value of the compliance with respect to $\boldsymbol{f}$, i.e.

$$c_{\max}(\boldsymbol{a}; \boldsymbol{p}) = \sup_{\boldsymbol{f} \in \mathbb{R}^n} \{c(\boldsymbol{a}; \boldsymbol{f}) \mid \boldsymbol{f} \in \mathcal{F}(\boldsymbol{p})\}, \tag{11}$$

which corresponds to the compliance at the most critical load among $\boldsymbol{f} \in \mathcal{F}(\boldsymbol{p})$. In the following we consider the minimization problem of $c_{\max}(\boldsymbol{a};\boldsymbol{p})$ defined in (11) in order to obtain the optimal topology of a robust truss.

We next show that the relation between p_j and the existence of the corresponding node is rewritten as the relationship among p_j and $t_1,\dots,t_m$, where t_i is the indicator of the existence of the ith member. Let $\mathcal{I}_k \subset \{1,\dots,m\}$ denote the set of indices of members which connect to the kth node. We denote by $\mathcal{J}_{\rm f} \subseteq \mathcal{J}$ the set of indices of the degrees of freedom of displacements of the node at which nonzero nominal load is applied, i.e. $\mathcal{J}_{\rm f} = \{j \in \mathcal{J}_k \mid \exists j \in \mathcal{J}_k : \tilde{f}_j \neq 0\}$. Define $\hat{p}_j : \mathbb{R}^m \to \mathbb{R}$ by

$$\hat{p}_j(\boldsymbol{t}) = \begin{cases} 1 & \text{if } j \in \mathcal{J}_{\rm f}, \\ 1 & \text{if } \exists i \in \{i \in \mathcal{I}_k \mid j \in \mathcal{J}_k\} : t_i = 1, \\ 0 & \text{otherwise.} \end{cases} \tag{12}$$

Then we see that Condition 1 is rewritten as

$$p_j = \hat{p}_j(\boldsymbol{t}), \quad j \in \mathcal{J}. \tag{13}$$

Now we give a rigorous definition of the robust topology optimization problem. We attempt to minimize the compliance in the worst case, $c_{\max}(\boldsymbol{a};\boldsymbol{p})$ defined in (11), over the conventional volume constraint and the positive lower bound constraints of the member cross-sectional areas. Note that p_j in $c_{\max}(\boldsymbol{a};\boldsymbol{p})$ is a function of $\boldsymbol{t}$ as shown in (13), and hence the loading conditions are considered to be dependent on the truss topology. From (6), (11), and (13), this optimization problem is formulated as

$$\begin{aligned} (\text{RTO}): \quad & \min_{\boldsymbol{a},\boldsymbol{t},\boldsymbol{p}} \quad c_{\max}(\boldsymbol{a};\boldsymbol{p}) && \text{(14a)} \\ & \text{s.t.} \quad p_j = \hat{p}_j(\boldsymbol{t}), \qquad \forall j, && \text{(14b)} \\ & \qquad a_i \begin{pmatrix} 1 \\ -1 \end{pmatrix} \leq t_i \begin{pmatrix} a_{\max} \\ -a_{\min} \end{pmatrix}, \quad \forall i, && \text{(14c)} \\ & \qquad \boldsymbol{l}^{\top}\boldsymbol{a} \leq \bar{V}, && \text{(14d)} \\ & \qquad \boldsymbol{t} \in \{0,1\}^m. && \text{(14e)} \end{aligned}$$

In the problem (14) it is difficult to deal with the objective function $c_{\max}(\boldsymbol{a};\boldsymbol{p})$ directly. We shall show that the inequality $\tau \geq c_{\max}(\boldsymbol{a};\boldsymbol{p})$ can be reduced to a linear matrix inequality in Lemma 3 below. We first state a simpler fact established in [9].

Lemma 2. *For the given $\boldsymbol{a} \in \mathbb{R}^m_+$, τ satisfies*

$$\tau \geq \sup_{\boldsymbol{u}\in\mathbb{R}^n,\ \boldsymbol{e}\in\mathbb{R}^{\ell}} \{2(Q\boldsymbol{e})^{\top}\boldsymbol{u} - \boldsymbol{u}^{\top}K(\boldsymbol{a})\boldsymbol{u} \mid 1 \geq \|\boldsymbol{e}\|\} \tag{15}$$

if and only if

$$\begin{pmatrix} \tau I & Q^{\top} \\ Q & K(\boldsymbol{a}) \end{pmatrix} \succeq O \tag{16}$$

holds.

A simple proof of Lemma 2 is given in appendix A for readers' convenience. The following lemma is a consequence of Lemma 2, and plays a key role to our tractable reformulation of (14).

Lemma 3. *For the given* $\boldsymbol{a} \in \mathbb{R}^m_+$ *and the given* $\boldsymbol{p} \in \{0,1\}^n$, τ *satisfies*

$$\tau \geq \sup_{\boldsymbol{f} \in \mathbb{R}^n} \{c(\boldsymbol{a};\boldsymbol{f}) \mid \boldsymbol{f} \in \mathcal{F}(\boldsymbol{p})\} \tag{17}$$

if and only if

$$\begin{pmatrix} \tau I & (\mathrm{diag}(\boldsymbol{p})Q)^\top \\ \mathrm{diag}(\boldsymbol{p})Q & K(\boldsymbol{a}) \end{pmatrix} \succeq O \tag{18}$$

holds.

Proof. From (2), (10), and (17), we obtain

$$\begin{aligned} \tau &\geq \sup_{\boldsymbol{f} \in \mathbb{R}^n} \{c(\boldsymbol{a};\boldsymbol{f}) \mid \boldsymbol{f} \in \mathcal{F}(\boldsymbol{p})\} \\ &= \sup_{\boldsymbol{f} \in \mathbb{R}^n,\ \boldsymbol{u} \in \mathbb{R}^n} \{2\boldsymbol{f}^\top \boldsymbol{u} - \boldsymbol{u}^\top K(\boldsymbol{a})\boldsymbol{u} \mid \boldsymbol{f} \in \mathcal{F}(\boldsymbol{p})\} \\ &= \sup_{\boldsymbol{e} \in \mathbb{R}^\ell,\ \boldsymbol{u} \in \mathbb{R}^n} \{2(\mathrm{diag}(\boldsymbol{p})Q\boldsymbol{e})^\top \boldsymbol{u} - \boldsymbol{u}^\top K(\boldsymbol{a})\boldsymbol{u} \mid 1 \geq \|\boldsymbol{e}\|\}. \end{aligned} \tag{19}$$

By comparing (15) and (19), we can see that the assertion of Lemma 3 is obtained by replacing Q in Lemma 2 with $\mathrm{diag}(\boldsymbol{p})Q$. □

Note that the condition (18) is a linear matrix inequality in terms of τ, $\boldsymbol{p}$, and $\boldsymbol{a}$.

In the problem (14) we next consider the nonlinear function $\hat{p}$ defined by (12). The following lemma implies that (13) is equivalently rewritten as some linear inequalities.

Lemma 4. *Suppose that*

$$\sup_{\boldsymbol{f} \in \mathbb{R}^n} \{c(\boldsymbol{a};\boldsymbol{f}) \mid \boldsymbol{f} \in \mathcal{F}(\boldsymbol{p})\} < +\infty \tag{20}$$

is satisfied. Then (13) *is equivalent to the following inequalities:*

$$0 \leq p_j \leq 1, \quad \forall i \in \{i \in \mathcal{I}_k \mid j \in \mathcal{J}_k\};\ \forall j \in \mathcal{J} \setminus \mathcal{J}_{\mathrm{f}}, \tag{21}$$

$$t_i \leq p_j, \quad \forall i \in \{i \in \mathcal{I}_k \mid j \in \mathcal{J}_k\};\ \forall j \in \mathcal{J} \setminus \mathcal{J}_{\mathrm{f}}, \tag{22}$$

$$p_j = 1, \quad \forall j \in \mathcal{J}_{\mathrm{f}}. \tag{23}$$

Proof. There exists nothing to be proved for $j \in \mathcal{J}_{\mathrm{f}}$. Moreover, it is easy to see that if p_j satisfies (13) then (21)–(23) hold. Hence, it suffices to show that p_j satisfies (13) if (20)–(22) are satisfied.

For $j \in \mathcal{J} \setminus \mathcal{J}_{\mathrm{f}}$, suppose that there exists an $i \in \{i \in \mathcal{I}_k \mid j \in \mathcal{J}_k\}$ such that $t_i = 1$. Then (22) is reduced to $1 \leq p_j$, from which and (21) we obtain $p_j = 1$. Thus (13) is satisfied.

Alternatively, suppose $t_i = 0$ for any $i \in \{i \in \mathcal{I}_k \mid j \in \mathcal{J}_k\}$. Note that this condition implies that no member is connected to the kth node. Then (22) is reduced to $0 \leq p_j$, which is redundant. If $p_j \neq 0$, then kth node is subjected to uncertain external loads. Since there exists no member connecting to the kth node, (20) is not satisfied in this case. Consequently, p_j must be 0, which satisfies (13). □

Lemma 4 implies that we can replace the constraint condition (14b) in (14) with (21)–(23) without changing the optimal solution, because (20) is satisfied at any feasible solution of (14). It should be emphasized that by using Lemma 4 we replace the binary constraint condition on p_j with the linear inequalities. Consequently, the problem (14) is equivalently rewritten as follows.

$$
\begin{aligned}
(\mathrm{RTO_c}): \quad & \min_{\tau, \boldsymbol{a}, \boldsymbol{t}, \boldsymbol{p}} \quad \tau && && \text{(24a)}\\
& \text{s.t.} \quad \begin{pmatrix} \tau I & (\mathrm{diag}(\boldsymbol{p})Q)^\top \\ \mathrm{diag}(\boldsymbol{p})Q & K(\boldsymbol{a}) \end{pmatrix} \succeq O, && && \text{(24b)}\\
& 0 \le p_j \le 1, \ t_i \le p_j, && \forall i \in \{ i \in \mathcal{I}_k \mid j \in \mathcal{J}_k \}; \ \forall j \in \mathcal{J} \setminus \mathcal{J}_{\mathrm{f}}, && \text{(24c)}\\
& p_j = 1, && \forall j \in \mathcal{J}_{\mathrm{f}}, && \text{(24d)}\\
& a_i \begin{pmatrix} 1 \\ -1 \end{pmatrix} \le t_i \begin{pmatrix} a_{\max} \\ -a_{\min} \end{pmatrix}, && \forall i, && \text{(24e)}\\
& \boldsymbol{l}^\top \boldsymbol{a} \le \bar{V}, && && \text{(24f)}\\
& \boldsymbol{t} \in \{0,1\}^m. && && \text{(24g)}
\end{aligned}
$$

We call the problem ($\mathrm{RTO_c}$) in (24) a 0–1MISDP (0–1 mixed integer semidefinite programming) problem, because it has binary constraint conditions on some variables and a linear matrix inequality constraint condition. Indeed, by relaxing $\boldsymbol{t} \in \{0,1\}^m$ in ($\mathrm{RTO_c}$) as $\boldsymbol{0} \le \boldsymbol{t} \le \boldsymbol{1}$ we obtain a conventional (linear) SDP problem.

3.2 Minimization of structural volume with robustness constraint

The minimization problem of the maximum compliance has been formulated as a 0–1MISDP in section 3.1. In this section, we show that the volume minimization problem with the specified worst-case compliance is also formulated as a 0–1MISDP.

We here consider the minimization problem of the structural volume with the upper bound constraint of the compliance in the worst case. Let $\bar{\tau}$ denote the specified upper bound of the compliance. The constraint condition on the maximum compliance is written as

$$\bar{\tau} \ge \sup_{\boldsymbol{f} \in \mathbb{R}^n} \{ c(\boldsymbol{a}; \boldsymbol{f}) \mid \boldsymbol{f} \in \mathcal{F}(\boldsymbol{p}) \}. \tag{25}$$

It follows from Lemma 3 that (25) is equivalently rewritten as

$$\begin{pmatrix} \bar{\tau} I & (\mathrm{diag}(\boldsymbol{p})Q)^\top \\ \mathrm{diag}(\boldsymbol{p})Q & K(\boldsymbol{a}) \end{pmatrix} \succeq O.$$

Hence, the minimization problem of the structural volume is formulated as

$$
\begin{aligned}
(\mathrm{RTO_v}): \quad & \min_{\boldsymbol{a},\boldsymbol{t},\boldsymbol{p}} \quad \boldsymbol{l}^\top \boldsymbol{a} && \text{(26a)}\\
& \text{s.t.} \quad \begin{pmatrix} \bar{\tau} I & (\mathrm{diag}(\boldsymbol{p})Q)^\top \\ \mathrm{diag}(\boldsymbol{p})Q & K(\boldsymbol{a}) \end{pmatrix} \succeq O, && \text{(26b)}\\
& 0 \le p_j \le 1, \ t_i \le p_j, \quad \forall i \in \{ i \in \mathcal{I}_k \mid j \in \mathcal{J}_k \}; \ \forall j \in \mathcal{J} \setminus \mathcal{J}_{\mathrm{f}}, && \text{(26c)}\\
& p_j = 1, \quad \forall j \in \mathcal{J}_{\mathrm{f}}, && \text{(26d)}\\
& a_i \begin{pmatrix} 1 \\ -1 \end{pmatrix} \le t_i \begin{pmatrix} a_{\max} \\ -a_{\min} \end{pmatrix}, \quad \forall i, && \text{(26e)}\\
& \boldsymbol{t} \in \{0,1\}^m. && \text{(26f)}
\end{aligned}
$$

Note that $(\mathrm{RTO_v})$ in (26) is a 0–1MISDP. In section 5.4 we solve $(\mathrm{RTO_v})$ for various values of r in order to investigate a trade-off relationship between the level of robustness and the optimal structural cost.

3.3 Proof of optimality

In this section we show that the optimal solution of $(\mathrm{RTO_c})$ presented in section 3.1 corresponds to the global optimal solution of the robust truss topology optimization problem. The same assertion for $(\mathrm{RTO_v})$ can be shown similarly, and hence is omitted.

For formulating $(\mathrm{RTO_c})$, we have introduced 0–1 variables p_j $(j \in \mathcal{J})$ so that the kth node is removed if $p_j = 0$ $(j \in \mathcal{J}_k)$. The remaining question on the optimality of $(\mathrm{RTO_c})$ is stated as follows. Consider a ground structure, which is referred to as the ground structure (A). Suppose that we solve $(\mathrm{RTO_c})$ for the ground structure (A) to find the optimal solution (B). Define the ground structure (C) by removing the vanishing nodes at (B) from the ground structure (A), i.e. the ground structure (C) consists of all the members of the ground structure (A) which do not connect to the vanishing nodes at (B). We then solve $(\mathrm{RTO_c})$ for the ground structure (C) to find the optimal solution (D). The question is whether (B) is equal to (D).

A positive answer to this question can be given based on Lemma 5 below. We assume without loss of generality that the kth node is removed at the solution (B) and that $\mathcal{J}_k = \{n\}$, i.e.

$$p_1 = \cdots = p_{n-1} = 1, \quad p_n = 0. \tag{27}$$

Since $\tilde{f}_n = 0$ from (13), there exists $\boldsymbol{g} \in \mathbb{R}^{n-1}$ satisfying

$$\tilde{\boldsymbol{f}} = \begin{pmatrix} \boldsymbol{g} \\ 0 \end{pmatrix}.$$

Define $Q' \in \mathbb{R}^{(n-1)\times(\ell-1)}$ by

$$Q' = (\boldsymbol{g}, r\boldsymbol{v}'_1, \dots, r\boldsymbol{v}'_{\ell-2}), \tag{28}$$

where $\boldsymbol{v}'_j$ $(j = 1, \dots, \ell-2)$ are orthonormal basis vectors of the orthogonal complement of $\boldsymbol{g}$. Then the uncertainty model of the external loads for the ground structure (C) is defined by

$$\bar{\mathcal{F}}' = \left\{ \begin{pmatrix} \boldsymbol{f}' \\ 0 \end{pmatrix} \mid \boldsymbol{f}' = Q'\boldsymbol{e}', \ \boldsymbol{e}' \in \mathbb{R}^{\ell-1}, \ 1 \ge \|\boldsymbol{e}'\| \right\}.$$

Note that the uncertainty model corresponding to the solution (B) is given by $\mathcal{F}(\boldsymbol{p})$ with (27).

Lemma 5. *If* (27) *is satisfied, then* $\mathcal{F}(\boldsymbol{p}) = \bar{\mathcal{F}}'$.

Proof. In (10) we see that $\{Q\boldsymbol{e} \mid 1 \geq \|\boldsymbol{e}\|\}$ represents an ellipsoid in the n-dimensional space. Observe that this ellipsoid does not depend on the choice of orthonormal basis vectors $\boldsymbol{v}_j$, and hence we obtain

$$\begin{aligned}
\{Q\boldsymbol{e} \mid 1 \geq \|\boldsymbol{e}\|\} &= \left\{ \begin{pmatrix} \tilde{\boldsymbol{f}}, r\boldsymbol{v}_1, r\boldsymbol{v}_2, \dots, r\boldsymbol{v}_{\ell-1} \end{pmatrix} \boldsymbol{e} \mid 1 \geq \|\boldsymbol{e}\| \right\} \\
&= \left\{ \begin{pmatrix} \boldsymbol{g} & r\boldsymbol{v}'_1 & \cdots & r\boldsymbol{v}'_{\ell-2} & \boldsymbol{0} \\ 0 & 0 & \cdots & 0 & r \end{pmatrix} \boldsymbol{e} \mid 1 \geq \|\boldsymbol{e}\| \right\} \\
&= \left\{ \begin{pmatrix} Q' & \boldsymbol{0} \\ \boldsymbol{0}^\top & r \end{pmatrix} \boldsymbol{e} \mid 1 \geq \|\boldsymbol{e}\| \right\},
\end{aligned} \tag{29}$$

where Q' is defined by (28). From (10) and (29), we obtain

$$\begin{aligned}
\mathcal{F}(\boldsymbol{p}) &= \{\boldsymbol{f} \mid \boldsymbol{f} = \mathrm{diag}(\boldsymbol{p})Q\boldsymbol{e},\ 1 \geq \|\boldsymbol{e}\|,\ p_1 = \cdots = p_{n-1} = 1,\ p_n = 0\} \\
&= \left\{ \boldsymbol{f} \mid \boldsymbol{f} = \begin{pmatrix} Q' & \boldsymbol{0} \\ \boldsymbol{0}^\top & 0 \end{pmatrix} \boldsymbol{e},\ 1 \geq \|\boldsymbol{e}\| \right\} \\
&= \left\{ \begin{pmatrix} \boldsymbol{f}' \\ 0 \end{pmatrix} \mid \boldsymbol{f}' = \begin{pmatrix} Q' & \boldsymbol{0} \end{pmatrix} \boldsymbol{e},\ 1 \geq \|\boldsymbol{e}\| \right\} \\
&= \left\{ \begin{pmatrix} \boldsymbol{f}' \\ 0 \end{pmatrix} \mid \boldsymbol{f}' = Q'\boldsymbol{e}',\ 1 \geq \|\boldsymbol{e}'\| \right\} \\
&= \bar{\mathcal{F}}',
\end{aligned}$$

which concludes the proof. □

Lemma 5 shows that if we change the set of existing nodes in the solution process of ($\mathrm{RTO_c}$), then the uncertainty model $\mathcal{F}(\boldsymbol{p})$ used in ($\mathrm{RTO_c}$) is automatically becomes equivalent to the uncertainty model $\bar{\mathcal{F}}'$ defined for a new ground structure with the remaining nodes. Hence, by solving ($\mathrm{RTO_c}$) we can obtain the global optimal solution in the sense that the solution (B) defined above is equal to the solution (D).

4 Branch-and-bound algorithm

We describe a branch-and-bound algorithm for finding the global optimum solution of ($\mathrm{RTO_c}$) in (24). An algorithm for ($\mathrm{RTO_v}$) can be designed similarly, and hence is omitted.

4.1 Relaxed problem

Since ($\mathrm{RTO_c}$) includes m binary variables, $t_1, \dots, t_m$, we construct a binary search tree based on the enumeration of all possible realization of $\boldsymbol{t}$. A node K of the binary tree is characterized by $\mathcal{T}_0^K$ and $\mathcal{T}_1^K$, where $\mathcal{T}_0^K$, $\mathcal{T}_1^K \subseteq \{1, \dots, m\}$ are the sets of indices of binary variables t_i's satisfying $\mathcal{T}_0^K \cap \mathcal{T}_1^K = \emptyset$. More precisely, $\mathcal{T}_0^K$ and $\mathcal{T}_1^K$ are defined by

$$\begin{aligned}
\mathcal{T}_0^K &= \{i \in \{1, \dots, m\} \mid t_i \text{ is fixed as } 0 \text{ at the node } K\}, \\
\mathcal{T}_1^K &= \{i \in \{1, \dots, m\} \mid t_i \text{ is fixed as } 1 \text{ at the node } K\}.
\end{aligned}$$

The subproblem to be solved at the node K is formulated as follows.

$$
\begin{aligned}
&(\mathrm{RTO_c})^K : \\
&\quad v^K = \min_{\tau, \boldsymbol{a}, \boldsymbol{t}, \boldsymbol{p}} \quad \tau && && \text{(30a)} \\
&\quad\quad \text{s.t.} \quad \begin{pmatrix} \tau I & (\mathrm{diag}(\boldsymbol{p})Q)^\top \\ \mathrm{diag}(\boldsymbol{p})Q & K(\boldsymbol{a}) \end{pmatrix} \succeq O, && && \text{(30b)} \\
&\quad\quad 0 \le p_j \le 1, \ t_i \le p_j, && \forall i \in \{ i \in \mathcal{I}_k \mid j \in \mathcal{J}_k \}; \ \forall j \in \mathcal{J} \setminus \mathcal{J}_{\mathrm{f}}, && \text{(30c)} \\
&\quad\quad p_j = 1, && \forall j \in \mathcal{J}_{\mathrm{f}}, && \text{(30d)} \\
&\quad\quad a_i \begin{pmatrix} 1 \\ -1 \end{pmatrix} \le t_i \begin{pmatrix} a_{\max} \\ -a_{\min} \end{pmatrix}, && \forall i, && \text{(30e)} \\
&\quad\quad \boldsymbol{l}^\top \boldsymbol{a} \le \bar{V}, && && \text{(30f)} \\
&\quad\quad t_i = 0, && i \in \mathcal{T}_0^K, && \text{(30g)} \\
&\quad\quad t_i = 1, && i \in \mathcal{T}_1^K, && \text{(30h)} \\
&\quad\quad 0 \le t_i \le 1, && i \notin \mathcal{T}_0^K \cup \mathcal{T}_1^K. && \text{(30i)}
\end{aligned}
$$

Let $(\tau^K, \boldsymbol{a}^K, \boldsymbol{t}^K, \boldsymbol{p}^K)$ and v^K denote the optimal solution and optimal value of the problem (30), respectively. We define $v^K = +\infty$ if the problem (30) is infeasible. Since (30) is a conventional SDP problem, we can solve (30) by using the primal-dual interior-point method efficiently [13]. Note that at the root node of the search tree, i.e. the node characterized by $\mathcal{T}_0^K = \mathcal{T}_1^K = \emptyset$, the problem (30) corresponds to a relaxation problem of $(\mathrm{RTO_c})$ in (24).

4.2 Upper bound

In the branch-and-bound method, we can prune the node K if $v^K > v^{\mathrm{U}}$, where v^{U} is an upper bound for the optimal value of $(\mathrm{RTO_c})$. Since a smaller value of v^{U} enables us to prune more nodes of the binary search tree, we attempt to propose a heuristic method for finding a good upper bound at the root node.

Observe that a feasible solution $(\mathrm{RTO_c})$ with a relatively small objective value may be obtained by choosing an appropriate set of existing members from the mechanical point of view. Such a candidate set may be obtained by solving a continuous relaxation of $(\mathrm{RTO_c})$ with $a_{\min} = 0$, and removing the members with small cross-sectional areas at the obtained optimal solution. Then we solve the shape optimization problem with the specified set of existing members to obtain an upper bound for $(\mathrm{RTO_c})$. This procedure is summarized as follows.

Algorithm 6 (heuristic method for obtaining an upper bound)**.**

Step 0: Choose a small constant ε, e.g. $\varepsilon = 10^{-5}$.

Step 1: Put $a_{\min} = 0$ and $\mathcal{T}_0^K = \mathcal{T}_1^K = \emptyset$. Solve (30) to find the optimal solution $(\tau^*, \boldsymbol{a}^*, \boldsymbol{t}^*, \boldsymbol{p}^*)$.

Step 2: Define $\mathcal{T}_0^*$, $\mathcal{T}_1^* \subseteq \{1, \dots, m\}$ by

$$\mathcal{T}_0^* = \{ i \mid a_i^* < \varepsilon \}, \quad \mathcal{T}_1^* = \{ i \mid a_i^* \ge \varepsilon \}.$$

Step 3: Put $(\mathcal{T}_0^K, \mathcal{T}_1^K) = (\mathcal{T}_0^*, \mathcal{T}_1^*)$, and solve (30) to find its optimal value v^{U} and optimal solution $(\overline{\tau}, \overline{\boldsymbol{a}}, \overline{\boldsymbol{t}}, \overline{\boldsymbol{p}})$.

4.3 Branching rule

In our branch-and-bound method, we essentially use the depth-first search [12] for selecting the next live node. Hence, after solving the subproblem $(\mathrm{RTO_c})^K$ at the node K, we usually generate some children nodes of K. Define $\hat{i}$ by

$$t_{\hat{i}}^K = \max_i \{ t_i^K \mid i \not\in \mathcal{T}_0^K \cup \mathcal{T}_1^K \}.$$

Let ε be a sufficiently small constant, e.g. $\varepsilon = 10^{-5}$, so that a variable which is less than ε at the optimal solution can be regarded as vanishing. We generate children nodes of the node K according to the following branching rule, which depends on the value of $t_{\hat{i}}^K$.

If $t_{\hat{i}}^K < \varepsilon$, i.e. if $t_i^K < \varepsilon$ $(\forall i \not\in \mathcal{T}_0^K \cup \mathcal{T}_1^K)$, then the solution $(\tau^K, \boldsymbol{a}^K, \boldsymbol{t}^K, \boldsymbol{p}^K)$ of $(\mathrm{RTO_c})^K$ can be regarded as being feasible for $(\mathrm{RTO_c})$, with small tolerance of numerical errors. In this case, we generate only one leaf node K_{leaf} as a child node of K, where K_{leaf} is associated with $\mathcal{T}_0^{K_{\mathrm{leaf}}}$ and $\mathcal{T}_1^{K_{\mathrm{leaf}}}$ defined by

$$\mathcal{T}_0^{K_{\mathrm{leaf}}} = \{1, \dots m\} \setminus \mathcal{T}_1^K, \quad \mathcal{T}_1^{K_{\mathrm{leaf}}} = \mathcal{T}_1^K.$$

The subproblem (30) to be solved at the node K_{leaf} satisfies $v^{K_{\mathrm{leaf}}} = v^K$.

Alternatively, if $t_{\hat{i}}^K \ge \varepsilon$ at the node K, then we generate two children nodes, K_+ and K_-, defined by

$$\mathcal{T}_0^{K_+} = \mathcal{T}_0^K, \quad \mathcal{T}_1^{K_+} = \mathcal{T}_1^K \cup \{\hat{i}\},$$
$$\mathcal{T}_0^{K_-} = \mathcal{T}_0^K \cup \{\hat{i}\}, \quad \mathcal{T}_1^{K_-} = \mathcal{T}_1^K.$$

As a heuristic strategy to accelerate the branch-and-bound method, we search K_+ before K_-. This strategy is motivated by the observation in Remark 7 below.

Remark 7. It is observed from our preliminary numerical experiments that the optimum value of the subproblem solved at the node K^+ is often smaller than that at the node K_-, i.e. $v^{K_+} < v^{K_-}$. This may be interpreted as follows. If the ith member does not contribute to reduce the maximum compliance, then t_i^K may attain to 0 as the result of optimization. Since $t_{\hat{i}}^K$ takes the maximum value among fractional t_i^K's, it seems that the $\hat{i}$th member has some contribution to reduce the maximum compliance, and hence the optimal value may be reduced with the existence of the $\hat{i}$th member. Since the better upper bound for the optimal value of $(\mathrm{RTO_c})$ may enable us to prune more nodes, it seems to be more efficient to visit K_+ before K_-. ■

In some cases, it is not necessary to visit the node K_+, and hence we immediately generate children nodes of K_+. Such a case is identified by Lemma 8 below.

Lemma 8. *If the optimal solution* $(\tau^K, \boldsymbol{a}^K, \boldsymbol{t}^K, \boldsymbol{p}^K)$ *of* $(\mathrm{RTO_c})^K$ *satisfies*

$$a_{\hat{i}}^K \ge a_{\min}, \qquad p_j^K = 1 \ (\forall j \in \mathcal{J}_k : \hat{i} \in \mathcal{I}_k), \tag{31}$$

then $v^{K_+} = v^K$.

Proof. Suppose that the assumption of Lemma 8 is satisfied. We construct the subproblem $(\mathrm{RTO_c})^{K_+}$ to be solved at the node K_+ by adding the following constraint conditions to $(\mathrm{RTO_c})^K$:

$$t_{\hat{i}} = 1, \tag{32}$$

$$p_j \geq t_{\hat{i}}, \quad \forall j \in \mathcal{J}_k : \hat{i} \in \mathcal{I}_k, \tag{33}$$

$$a_{\min} \leq a_{\hat{i}} \leq a_{\max}. \tag{34}$$

It is easy to see that $\boldsymbol{a}^K$, $\boldsymbol{t}^K$, and $\boldsymbol{p}^K$ satisfy (33) and (34). Define $\tilde{\boldsymbol{t}}^K$ by

$$\tilde{t}_i^K = \begin{cases} t_i^K & \text{for } i \neq \hat{i}. \\ 1 & \text{for } i = \hat{i}, \end{cases}$$

so that $\tilde{\boldsymbol{t}}^K$ satisfies (32). Then we see that $(\tau^K, \boldsymbol{a}^K, \tilde{\boldsymbol{t}^K}, \boldsymbol{p}^K)$ is feasible for $(\mathrm{RTO_c})^{K_+}$. Since the objective function of $(\mathrm{RTO_c})^{K_+}$ is independent of $\boldsymbol{t}$, the inequality $v_{K_+} \leq v_K$ is obtained. On the other hand, since K_+ is a child node of K, we have $v_{K_+} \geq v_K$, which concludes the proof. □

As a consequence of Lemma 8, if the condition (31) is satisfied at the node K_+, then we do not visit K_+ but generate two children nodes of K_+ by putting $K := K_+$ in the branching rule presented above.

4.4 Description of algorithm

With the details presented in sections 4.1–4.3, our branch-and-bound method for the 0–1MISDP (14) is described as follows.

Algorithm 9 (branch-and-bound algorithm for $(\mathrm{RTO_c})$)**.**

- **Step 1:** Define the root node, K_0, of the search tree by $\mathcal{T}_0^{K_0} = \mathcal{T}_1^{K_0} = \emptyset$.
- **Step 2:** Compute v^{U} and $\overline{\boldsymbol{a}}$ by using Algorithm 6.
- **Step 3:** Select a node K which has not been visited in the search tree. If none exists, then go to Step 7.
- **Step 4:** Solve $(\mathrm{RTO_c})^K$ at the node K. Let v^K and $(\tau^K, \boldsymbol{a}^K, \boldsymbol{t}^K, \boldsymbol{p}^K)$ denote its optimal value and optimal solution, respectively. If $v^K \geq v^{\mathrm{U}}$, then go to Step 3.
- **Step 5:** If the node K is a leaf node, then update $v^{\mathrm{U}} \leftarrow v^K$ and $\overline{\boldsymbol{a}} \leftarrow \boldsymbol{a}^K$. Go to Step 3.
- **Step 6:** Generate some children nodes of the node K by applying the branching rule presented in section 4.3. Go to Step 3.
- **Step 7:** Declare $\overline{\boldsymbol{a}}$ as the optimal solution of $(\mathrm{RTO_c})$, and stop.

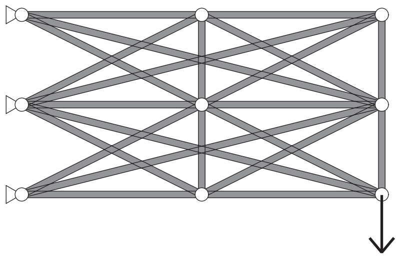

(a) The ground structure.

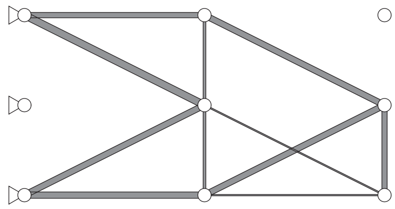

(b) The optimal solution of $(\mathrm{RTO_c})$.

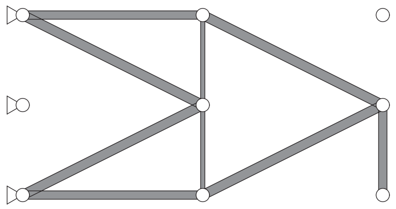

(c) The optimal solution of (TO).

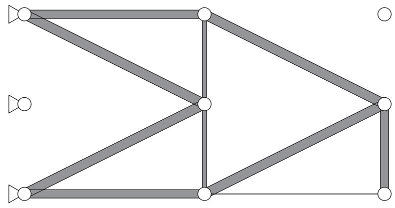

(d) The optimal solution of $(\mathrm{RTO_c})$ with $a_{\min} = 0$.

Figure 3: A 22-member truss example.

5 Numerical experiments

In this section we show numerical examples of the robust topology optimization of various trusses. Computation has been carried out on Core2 Duo (2.00 GHz with 1.99 GB memory) with MATLAB Ver. R2007b [22]. We solve linear SDP problems by using SeDuMi Ver. 1.05 [21], which implements the primal-dual interior-point method.

In sections 5.1–5.3 we solve $(\mathrm{RTO_c})$, while $(\mathrm{RTO_v})$ is solved in section 5.4 in order to study a relationship between the level of robustness and the optimal structural volume. In the following examples, the lengths of horizontal and vertical members of trusses are 100 cm and 50 cm, respectively, $a_{\min} = 10\,\mathrm{cm}^2$, $a_{\max} = 10^3\,\mathrm{cm}^2$, and the elastic modulus is 200 GPa. Note that the upper bound constraints of the member cross-sectional areas are inactive at the optimal solutions of all the following examples. The level of uncertainty is $r = \|\tilde{\boldsymbol{f}}\|/10$ in the examples of sections 5.1–5.3.

5.1 22-member truss

Consider a 22-member plane truss illustrated in Figure 3 (a). The three nodes on the left side are fixed. As the nominal external load $\tilde{\boldsymbol{f}}$, the bottom-right node is loaded by the vertical force of 1 kN. The upper bound of structural volume is $\bar{V} = 8.3818 \times 10^4\,\mathrm{cm}^3$.

The optimal solution obtained by solving $(\mathrm{RTO_c})$ is illustrated in Figure 3 (b), where the width of each member is proportional to its cross-sectional area. The computational results are listed in Table 1. Here, $c_{\max}$ denotes the maximal compliance defined by (11) at the optimal design, 'Nodes' is the number of nodes of the binary search tree visited by Algorithm 9, and '$c_{\max}^{\mathrm{U}}$' is the maximal compliance of a solution obtained by Algorithm 6. For comparison the optimal solution of (TO) is illustrated in Figure 3 (c). Notice here that (TO) can be regarded as a particular case of $(\mathrm{RTO_c})$ with $r = 0$. Figure 3 (d) shows the optimal solution of $(\mathrm{RTO_c})$ with $a_{\min} = 0$.

It is observed in Table 1 that $\operatorname{rank} D < n$ for the optimal solution of (TO), i.e. the nominal

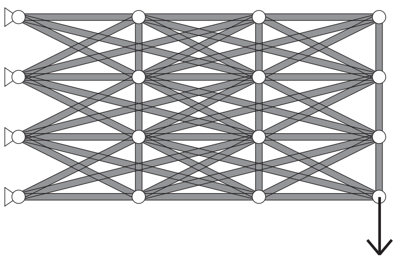

(a) The ground structure.

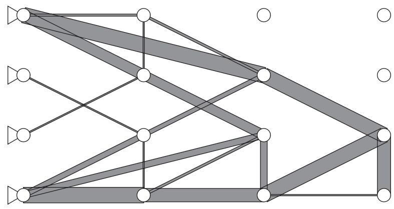

(b) The optimal solution of ($\mathrm{RTO_c}$).

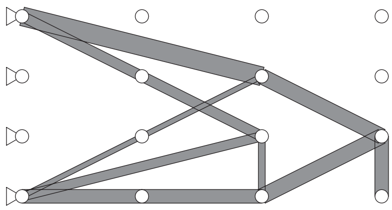

(c) The optimal solution of (TO).

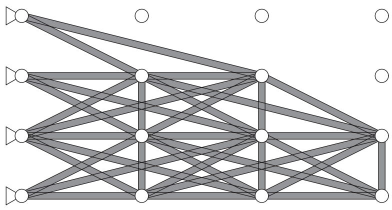

(d) The ground structure obtained from Figure 4 (c).

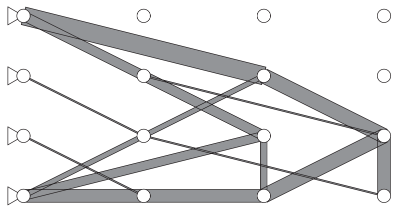

(e) The solution obtained from the ground structure in Figure 4 (e)

Figure 4: A 51-member truss example.

optimal solution is kinematically unstable. In contrast, we see that $\mathrm{rank}\, D = n$ for the optimal solution of ($\mathrm{RTO_c}$), and hence the solution of the robust optimization problem is kinematically stable.

It is observed in Figure 3 (d) that the optimal solution of the robust optimization with $a_{\min} = 0$ has a very thin member. The cross-sectional area of this member is $0.15\,\mathrm{cm}^2$, which is not acceptable from the practical point of view. In addition, the topology of Figure 3 (d) is different from that of Figure 3 (b), i.e. a diagonal member in Figure 3 (b) does not appear in Figure 3 (d). Such a difference of optimal topologies may be explained as follows. If we solve the problem without positive lower bound for member cross-sectional areas, there may exist two types of thin members at the optimal solution. One is a member which is necessary for minimizing the maximum compliance, and the other is a member which is unnecessary but has a positive small cross-sectional area because of numerical error. We usually remove members in the second type by using a small positive threshold. However, if the cross-sectional areas of members in both types are very close, some members in the first type are also removed. Thus, a diagonal member has been removed in Figure 3 (d), although $c_{\max}$ becomes very large without that member. In contrast, in Figure 3 (b), the necessary members are thick enough to be distinguished from unnecessary members.

It is emphasized that Algorithm 9 can find the optimal solution of (TO) after visiting only one node in the binary search tree. This is because the optimal solution of (TO) is found by Algorithm 6, which is carried out for finding a good upper bound for (TO). Accordingly, we may

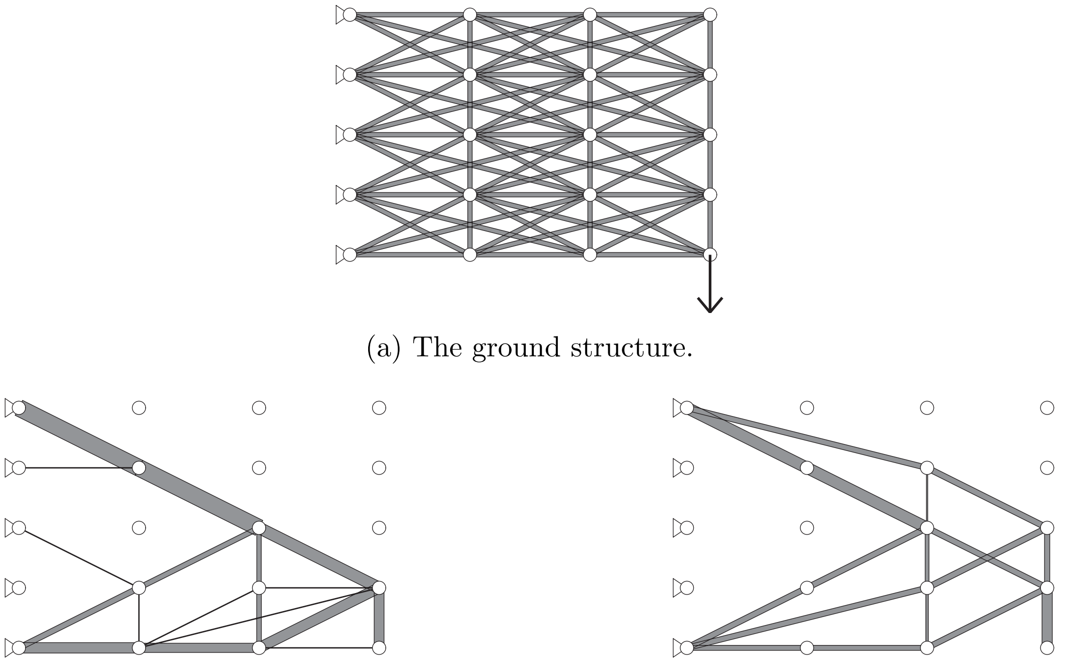

(a) The ground structure.

(b) The optimal solution of ($\mathrm{RTO_c}$).

(c) The optimal solution of (TO).

Figure 5: A 67-member truss example.

conclude that the upper-bound solution obtained by Algorithm 6 accelerates the branch-and-bound method (Algorithm 9) drastically.

5.2 51-member truss

Consider a ground structure illustrated in Figure 4 (a). All the four nodes on the left side are fixed, while the bottom-right node is loaded by the nominal vertical force of 1 kN. The upper bound of structural volume is $\bar{V} = 1.2273 \times 10^5\,\mathrm{cm}^3$. The optimal solutions of ($\mathrm{RTO_c}$) and (TO) are illustrated in Figures 4 (b) and (c), respectively, and the computational results are listed in Table 2.

The structure shown in Figure 4 (b) is kinematically stable, because it satisfies $\mathrm{rank}\, D = n$. In contrast, the structure in Figure 4 (c) is kinematically unstable.

Observe that the optimal solution of ($\mathrm{RTO_c}$) in Figure 4 (b) has one additional free node compared with the optimal solution of (TO) in Figure 4 (c). Figure 4 (d) depicts a ground structure suggested by Figure 4 (c). After solving (TO), we may consider the ground structure shown in Figure 4 (d) and solve the robust optimization problem without considering the possible vanishment of nodes, which is a procedure suggested in [9]. Figure 4 (e) illustrates the optimal solution of ($\mathrm{RTO_c}$) for the ground structure in Figure 4 (d) under the condition such that all the nodes should exist. The maximal compliance of the structure in Figure 4 (e) is $6.3177\,\mathrm{kN \cdot cm}$, which is larger than that of the optimal solution of ($\mathrm{RTO_c}$) in Figure 4 (b). Thus, a heuristic method suggested in [9] cannot find the global optimal solution of the robust topology optimization problem in general, and hence it is necessary to solve ($\mathrm{RTO_c}$) which we have proposed.

Table 1: Computational results of the 22-member truss example.

	$c_{\max}$ (kN · cm)	rank D	n	Nodes	CPU (sec)	$c_{\max}^{\mathrm{U}}$ (kN · cm)
(TO)	6.3516	9	10	1	0.6	6.3516
($\mathrm{RTO_c}$)	6.5457	10	10	24	6.3	6.5648

Table 2: Computational results of the 51-member truss example.

	$c_{\max}$ (kN · cm)	rank D	n	Nodes	CPU (sec)	$c_{\max}^{\mathrm{U}}$ (kN · cm)
(TO)	5.8667	12	16	20	15.8	5.9712
($\mathrm{RTO_c}$)	6.0644	18	18	366	369.1	6.1876

5.3 67-member truss

Consider a moderately large example of the ground structure illustrated in Figure 5 (a). All the five nodes on the left side are fixed, while the bottom-right node is loaded by the nominal vertical force of 1 kN. The upper bound of structural volume is $\bar{V} = 1.6164 \times 10^5\,\mathrm{cm}^3$. The optimal solutions of ($\mathrm{RTO_c}$) and (TO) are illustrated in Figures 5 (b) and (c), respectively. The computational results are listed in Table 3. It is emphasized that the topology, as well as the set of remaining nodes, of Figure 5 (b) is entirely different from that of Figure 5 (c).

5.4 Level of uncertainty and optimal structural volume

In sections 5.1–5.3 we have supposed that the level of uncertainty, r, in (7) is fixed. In this section we solve ($\mathrm{RTO_v}$) for various values of r in order to see the relationship among the structural volume, the level of uncertainty, and the topology of robust optimal solution.

Consider the ground structure investigated in section 5.1. Figure 6 (a) plots a relation between the level of robustness, r, and the structural volume of the robust optimal solutions, where $\bar{\tau} = 10.0\,\mathrm{kN \cdot cm}$ in ($\mathrm{RTO_v}$). As r changes, the optimal topology changes in the four types illustrated in Figures 6 (b)–(e).

When r is small enough, the optimal topology is similar to the topology of the optimal solution without considering uncertainties, i.e. $r = 0$. As r becomes larger, the optimal topology changes so as to decrease its number of remaining members and increase the cross-sectional areas of existing members. When r becomes much larger, the optimal topology has fewer nodes so that the number of nodes subjected to uncertain loads decreases. Note that the curve in Figure 6 (a) is not continuous at $r = 0$. This is because we consider positive lower bounds for the member cross-sectional areas. From Figure 6 we can see the relationship among the structural volume, the level of uncertainty, and the topology of robust optimal solution. Such a figure may help us to make decisions incorporating the trade-off relation between the level of robustness and the structural cost.

Table 3: Computational results of the 67-member truss example.

	$c_{\max}$ (kN · cm)	rank D	n	Nodes	CPU (sec)	$c^{\mathrm{U}}_{\max}$ (kN · cm)
(TO)	3.4105	16	20	1	3.8	3.4105
($\mathrm{RTO_c}$)	3.5585	17	16	8396	14300.0	3.7587

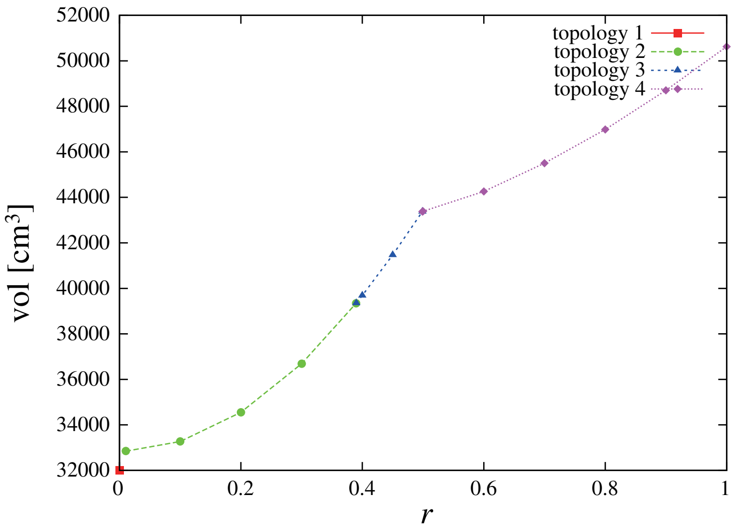

(a) Variation of the optimal structural volume with respect to the level of uncertainty.

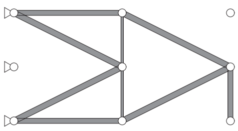

(b) Topology 1.

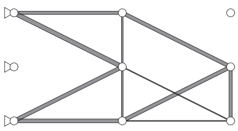

(c) Topology 2.

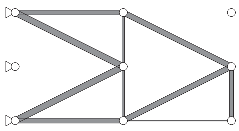

(d) Topology 3.

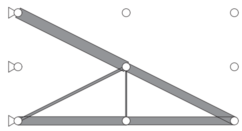

(e) Topology 4.

Figure 6: Relationship among the level of uncertainty, optimal structural volume, and optimal topology of the 22-member truss example.

6 Conclusions

We have presented a new formulation of the robust truss topology optimization problem considering the load uncertainties. The non-stochastic uncertainty model of external loads has been considered, and the robust optimization problem has been formulated as the minimization of the maximal compliance corresponding to the most critical load. We have proposed a design-dependent uncertainty model of external forces in order to deal with the variation of truss topology rigorously in the process of optimization. By introducing binary variables representing the existence of members, it has been shown that the robust topology optimization can be formulated as a 0–1MISDP (0–1mixed integer semidefinite programming) problem. We solve the 0–1MISDP by using the branch-and-bound method, at each iteration of which we solve a linear SDP problem by using the primal-dual interior-point method. For acceleration of the branch-and-bound method, we have proposed a heuristic method for finding an upper bound solution, as well as a particular branching rule designed for the robust truss optimization. Robust optimal solutions have been computed for various trusses by using the proposed algorithm.

A Proof of Lemma 2

Proof. Observe that (15) is equivalent to

$$\tau - 2(Q\boldsymbol{e})^\top \boldsymbol{u} + \boldsymbol{u}^\top K(\boldsymbol{a})\boldsymbol{u} \geq 0, \quad \forall \boldsymbol{u} \in \mathbb{R}^n,\ \forall \boldsymbol{e} \in \mathbb{R}^\ell : \|\boldsymbol{e}\| \leq 1. \tag{35}$$

Let $\lambda > 0$. By multiplying both hand-sides of (35) by λ^2 we obtain

$$\tau\lambda^2 - 2(Q\lambda\boldsymbol{e})^\top (\lambda\boldsymbol{u}) + (\lambda\boldsymbol{u})^\top K(\boldsymbol{a})(\lambda\boldsymbol{u}) \geq 0, \quad \forall \boldsymbol{u} \in \mathbb{R}^n,\ \forall \boldsymbol{e} \in \mathbb{R}^\ell : \|\boldsymbol{e}\| \leq 1. \tag{36}$$

Define $\tilde{\boldsymbol{e}}$ and $\boldsymbol{y}$ by

$$\tilde{\boldsymbol{e}} = \lambda\boldsymbol{e}, \tag{37}$$

$$\boldsymbol{y} = \lambda\boldsymbol{u}. \tag{38}$$

Then, for any $\lambda > 0$, we see that (36) is equivalently reduced to

$$\tau\lambda^2 - 2(Q\tilde{\boldsymbol{e}})^\top \boldsymbol{y} + \boldsymbol{y}^\top K(\boldsymbol{a})\boldsymbol{y} \geq 0, \quad \forall \boldsymbol{u} \in \mathbb{R}^n,\ \forall \boldsymbol{e} \in \mathbb{R}^\ell : \|\boldsymbol{e}\| \leq \lambda \tag{39}$$

with (37) and (38).

In (39) put $\lambda = \|\tilde{\boldsymbol{e}}\|$ as a specific value. Then (39) is reduced to

$$\tau(\tilde{\boldsymbol{e}}^\top \tilde{\boldsymbol{e}}) - 2(Q\tilde{\boldsymbol{e}})^\top \boldsymbol{y} + \boldsymbol{y}^\top K(\boldsymbol{a})\boldsymbol{y} \geq 0, \quad \forall \boldsymbol{y} \in \mathbb{R}^n,\ \forall \tilde{\boldsymbol{e}} \in \mathbb{R}^\ell, \tag{40}$$

which is equivalently rewritten as

$$\begin{pmatrix} \tilde{\boldsymbol{e}} \\ \boldsymbol{y} \end{pmatrix}^\top \begin{pmatrix} \tau I & Q^\top \\ Q & K(\boldsymbol{a}) \end{pmatrix} \begin{pmatrix} \tilde{\boldsymbol{e}} \\ \boldsymbol{y} \end{pmatrix} \geq 0, \quad \forall \boldsymbol{y} \in \mathbb{R}^n,\ \forall \tilde{\boldsymbol{e}} \in \mathbb{R}^\ell.$$

Consequently, if (15) is satisfied, then (16) holds.

We next show that (16) implies (15). Observe that if (16) is satisfied, then (40) holds. Choose λ satisfying $\lambda^2 \geq \tilde{\boldsymbol{e}}^\top \tilde{\boldsymbol{e}}$ in (40). Then, for any $\boldsymbol{y} \in \mathbb{R}^n$ and $\tilde{\boldsymbol{e}} \in \mathbb{R}^\ell$ we have

$$\begin{aligned} 0 &\leq \tau(\tilde{\boldsymbol{e}}^\top \tilde{\boldsymbol{e}}) - 2(Q\tilde{\boldsymbol{e}})^\top \boldsymbol{y} + \boldsymbol{y}^\top K(\boldsymbol{a})\boldsymbol{y} \\ &\leq \tau\lambda^2 - 2(Q\tilde{\boldsymbol{e}})^\top \boldsymbol{y} + \boldsymbol{y}^\top K(\boldsymbol{a})\boldsymbol{y}. \end{aligned} \tag{41}$$

Note that the last inequality in (41) follows the facts that $\tau \geq 0$ in (16) and $\lambda^2 \geq \tilde{\boldsymbol{e}}^\top \tilde{\boldsymbol{e}}$. Thus (39) holds and, equivalently, (15) is satisfied, which concludes the proof of Lemma 2. □

Acknowledgments

This work is partially supported by a Grant-in-Aid for Scientific Research from the Ministry of Education, Culture, Sports, Science and Technology of Japan.

References

[1] Achtziger, W., Bendsøe, M., Ben-Tal, A., Zowe, J.: Equivalent displacement based formulations for maximum strength truss topology design. *IMPACT of Computing in Science and Engineering*, **4**, 315–345 (1992).

[2] Achtziger, W., Stolpe, M.: Truss topology optimization with discrete design variables — Guaranteed global optimality and benchmark examples. *Structural and Multidisciplinary Optimization*, **34**, 1–20 (2007).

[3] Achtziger, W., Stolpe, M.: Global optimization of truss topology with discrete bar areas — Part I: Theory of relaxed problems. *Computational Optimization and Applications*, **40**, 247–280 (2008).

[4] Achtziger, W., Stolpe, M.: Global optimization of truss topology with discrete bar areas — Part II: Implementation and numerical results. *Computational Optimization and Applications*. doi: 10.1007/s10589-007-9152-7.

[5] Au, F.T.K., Cheng, Y.S., Tham, L.G., Zheng, G.W.: Robust design of structures using convex models. *Computers & Structures*, **81**, 2611–2619 (2003).

[6] Bendsøe, M.P., Ben-Tal, A., Zowe, J.: Optimization methods for truss geometry and topology design. *Structural and Multidisciplinary Optimization*, **7**, 141–159 (1994).

[7] Ben-Haim, Y.: *Information-gap Decision Theory: Decisions under Severe Uncertainty (2nd ed.)*. Academic Press, London (2006).

[8] Ben-Haim, Y., Elishakoff, I.: *Convex Models of Uncertainty in Applied Mechanics*. Elsevier, New York (1990).

[9] Ben-Tal, A., Nemirovski, A.: Robust truss topology design via semidefinite programming. *SIAM Journal on Optimization*, **7**, 991–1016 (1997).

[10] Beyer, H.-G., Sendhoff, B.: Robust optimization — A comprehensive survey. *Computer Methods in Applied Mechanics and Engineering*, **196**, 3190–3218 (2007).

[11] Cherkaev, E., Cherkaev, A.: Minimax optimization problem of structural design. *Computers & Structures*, **86**, 1426–1435 (2008).

[12] Clausen, J., Perregaard, M.: On the best search strategy in parallel branch-and-bound: best-first search versus lazy depth-first search. *Annals of Operations Research*, **90**, 1–17 (1999).

[13] Helmberg, C.: Semidefinite programming. *European Journal of Operational Research*, **137**, 461–482 (2002).

[14] Jarre, F., Kočvara, M., Zowe, J.: Optimal truss topology design by interior-point methods. *SIAM Journal on Optimization*, **8**, 1084–1107 (1998).

[15] Kanno, Y., Takewaki, I.: Sequential semidefinite program for robust truss optimization based on robustness functions associated with stress constraints. *Journal of Optimization Theory and Applications*, **130**, 265–287 (2006).

[16] Kočvara, M., Zowe, J., Nemirovski, A.: Cascading — an approach to robust material optimization. *Computers & Structures*, **76** 431–442, (2000).

[17] Korte, B., Vygen, J.: *Combinatorial Optimization (2nd ed.)*. Springer-Verlag, Berlin (2002).

[18] Matsuda, Y., Kanno, Y.: Robustness analysis of structures based on plastic limit analysis with uncertain loads. *Journal of Mechanics of Materials and Structures*, **3**, 213–242 (2008).

[19] Ohsaki, M., Katoh, N.: Topology optimization of trusses with stress and local nodal stability and member intersection. *Structural and Multidisciplinary Optimization*, **29**, 190–197 (2005).

[20] Pantelides, C.P., Ganzerli, S.: Design of trusses under uncertain loads using convex models. *Journal of Structural Engineering (ASCE)*, **124**, 318–329 (1998).

[21] Sturm, J.F.: Using SeDuMi 1.02, a MATLAB toolbox for optimization over symmetric cones. *Optimization Methods and Software*, **11/12**, 625–653 (1999).

[22] The MathWorks, Inc.: *Using MATLAB*. The MathWorks, Inc., Natick (2009).

[23] Zang, C., Friswell, M.I., Mottershead, J.E.: A review of robust optimal design and its application in dynamics. *Computers & Structures*, **83**, 315–326 (2005).